Available online at www.sciencedirect.com
ScienceDirect
Chemical Physics Letters 438 (2007) 14–19
CHEMICAL PHYSICS LETTERS
www.elsevier.com/locate/cplett

Vibrationally resolved nitrogen K-shell photoelectron spectra of the dinitrogen oxide molecule: Experiment and theory

M. Ehara [a,*], R. Tamaki [a], H. Nakatsuji [a,b], R.R. Lucchese [c,d], J. Söderström [c,e], T. Tanaka [g], M. Hoshino [g], M. Kitajima [g], H. Tanaka [g], A. De Fanis [f], K. Ueda [c]

[a] Department of Synthetic Chemistry and Biological Chemistry, Graduate School of Engineering, Kyoto University, Nishikyo-ku, Katsura, Kyoto 615-8510, Japan
[b] Quantum Chemistry Research Institute, 58-8 Mikawa, Momoyama-cho, Fushimi-ku, Kyoto 612-8029, Japan
[c] Institute of Multidisciplinary Research for Advanced Materials, Tohoku University, Sendai 980-8577, Japan
[d] Department of Chemistry, Texas A&M University, College Station, TX 77843-3255, USA
[e] Department of Physics, Uppsala University, P.O. Box 530, SE-751 21 Uppsala, Sweden
[f] SPring-8/JASRI, Koto 1-1, Sayo-gun, Hyogo 679-5198, Japan
[g] Department of Physics, Sophia University, Tokyo 102-8554, Japan

Received 24 December 2006; in final form 16 February 2007
Available online 25 February 2007

Abstract

Vibrationally resolved N_c and N_t K-shell photoelectron spectra of the dinitrogen oxide have been studied experimentally and theoretically. Vibrational frequencies for the N_c and N_t 1s ionized states obtained from the 2D potential surfaces computed by the CCSD(T) method within the equivalent core approximation reasonably agree with the experimental values. Experimental relative intensities of the vibrational structure are reasonably reproduced by the multi-channel Schwinger configuration interaction method (MCSCI) with the computed 2D potential surfaces. Improved relaxed geometries of these core–hole states are obtained from fitting the experimental spectra using the MCSCI calculations and regarding the bond lengths as fitting parameters.

1. Introduction

Vibrational excitation often accompanies the photoionization of a molecule [1,2]. This is also the case for core-level photoemission [3–5], even though the core electrons are non-bonding and thus a significant change in geometry may not be expected. Reproduction of the vibrational structure observed in the core-level photoelectron spectra has been a challenge to ab initio theory [5–7]. Recent developments of the third generation synchrotron radiation light sources, soft X-ray monochromators and high-resolution electron spectroscopy have renewed interest in core-level photoelectron spectroscopy study of free molecules [5,8,9]. Indeed vibrationally-resolved core-level photoelectron spectra recorded at the third generation synchrotron radiation facilities have been providing us with excellent benchmarks for ab initio calculations and the information about the geometry relaxation of the core ionized states [5,9–16].

In the present Letter, we report the experimental and theoretical investigation on the vibrational structure of the N 1s photoelectron spectra of the N_2O molecule. N_2O is a linear molecule that has two nitrogen atoms in different sites, labeled as center (N_c) and terminal (N_t). We have successfully observed vibrational structures both for the N_c and N_t core-level photoelectron spectra using monochromatized synchrotron radiation as a light source, as reported elsewhere without details [17]. In the present work, the vibrational spectra are theoretically studied by calculating the two-dimensional (2D) potential energy

* Corresponding author. Fax: +81 75 383 2741.
E-mail addresses: ehara@sbchem.kyoto-u.ac.jp (M. Ehara), ueda@tagen.tohoku.ac.jp (K. Ueda).

0009-2614/$ - see front matter © 2007 Elsevier B.V. All rights reserved.
doi:10.1016/j.cplett.2007.02.057

surfaces. The coupled-cluster singles and doubles with non-iterative triples (CCSD(T)) method is adopted within the equivalent core approximation (ECA). The ECA has been frequently used for the analysis and simulation of the vibrationally resolved spectra that appear in the core–hole states. Simulations based on the ECA often reproduce well the vibrational spectra providing reliable assignments [6,18], though a great care is necessary to use the ECA, because it may cause a significant error in some cases [18]. Recently, an improved ECA was developed to calculate core–hole states more accurately [19,20]. Relative intensities for vibrationally resolved photoelectron spectra are then calculated using the multi-channel Schwinger configuration interaction method (MCSCI) [21–23] within the adiabatic approximation and using the computed 2D potential surfaces. Finally, we extract the equilibrium geometries of the core ionized state from the experimental data, employing the MCSCI and regarding the equilibrium bond lengths as fitting parameters.

2. Experimental

The measurements were carried out at the c-branch of the beam line 27SU at SPring-8, a third generation synchrotron radiation facility with an 8-GeV storage ring in Japan. The figure-8 undulator installed in this beam line produces high-intensity linearly polarized soft X-rays. When integer order (i.e. 1st, 2nd, etc.) harmonics of the undulator radiation are chosen, the light is horizontally polarized. The half-integer (i.e. 0.5^{th}, 1.5^{th}, etc.) harmonics provide vertically polarized light [24]. The radiation was guided to a high-resolution soft X-ray monochromator installed in the c-branch. A more detailed description of the beam line and the monochromator can be found elsewhere [25,26]. The ejected electrons were analyzed with an SES-2002 electron energy analyzer (Gammadata-Scienta) equipped with a gas cell: the analyzer was mounted with the lens axis in the horizontal direction [27]. The pressure in the chamber was kept at $\sim 4.5 \times 10^{-5}$ Pascal throughout the experiment. Both horizontally and vertically polarized light from the undulator was used. The degree of linear polarization was determined by observing the Ne 2s and 2p photolines and confirmed to be greater than 0.98 with the present setting of the optics [28]. In the analysis, we thus assume complete polarization at the photon energies employed and obtain angle-independent electron emission intensity as $I(0°) + 2 \times I(90°)$, with $I(0°)$ and $I(90°)$ being the spectral intensity of the electron emission measured for the horizontal and vertical polarization, respectively.

3. Theoretical

The ground state electronic configuration of the N_2O molecule is

$$(1\sigma)^2(2\sigma)^2(3\sigma)^2(4\sigma)^2(5\sigma)^2(6\sigma)^2(1\pi)^4(7\sigma)^2(2\pi)^4(^1\Sigma^+).$$

Here, 1σ, 2σ and 3σ correspond to the O 1s, N_c 1s, and N_t 1s core orbitals, respectively. The N_2O molecule has four vibrational modes, two stretching modes $(v_1', 0, 0)$ and $(0, 0, v_3')$ and a doubly-degenerate bending mode $(0, v_2', 0)$. $(v_1', 0, 0)$ and $(0, 0, v_3')$ are similar to symmetric and antisymmetric vibrations, respectively, in CO_2 and thus are often called quasi-symmetric and quasi-antisymmetric stretching vibrations. Potential energy surfaces of the ground, N_c and N_t 1s core ionized states were calculated for the two dimensional surfaces along q_1 and q_3, i.e., the direction of the normal coordinates corresponding to the quasi-symmetric (v_1') and quasi-antisymmetric (v_3') stretching vibrational motions, in the regions of $R_{NN} = 0.9$–1.45 Å and $R_{NO} = 0.9$–1.45 Å. To calculate the 2D potential energy surface of the core–hole states, the ECA was adopted. For N_c and N_t 1s ionized states, the ground states of NOO^+ and ONO^+, respectively, were calculated using the CCSD(T) method. The basis sets were correlation consistent polarized valence triple zeta (cc-pVTZ) basis sets proposed by Dunning, namely [4s3p2d1f] [29]. The CCSD(T) calculations were executed with the GAUSSIAN 03 suite of programs [30].

The calculated potential energy surfaces were fitted with the two dimensional Morse functions [12] and the vibrational analysis was performed. For calculating the spectrum, vibrational wave functions and the Franck–Condon factors were obtained by the grid method, in which Lanczos algorithm was adapted for the diagonalization.

For a direct comparison between theory and experiment, we have computed vibrationally specific photoionization cross sections using the MCSCI method [21–23]. The details of these calculations will be given elsewhere [31] . Briefly, fixed-nuclei photoionization dipole matrix elements are obtained including two electronic channels that correspond to ionization leading to the N_t and N_c hole states of N_2O^+. These matrix elements are obtained on a grid of $\{R(NN), R(NO)\}$ points. The vibrationally specific matrix elements are then obtained as a 2D integral of the geometry dependent dipole matrix elements multiplied by the vibrational wave functions for the ground and ionized states. Ratios of the cross sections obtained from the resulting matrix elements then yield the ratios that can be compared to the experimental data.

4. Results

The N_c 1s photoelectron spectrum of N_2O, in the form of $I(0°) + 2 \times I(90°)$, measured at a photon energy $h\nu = 450$ eV, is shown in Fig. 1, together with a least-squares curve fitting decompositions into a vibrational progression. Both stretching modes v_1' and v_3' can in principle be excited via the N_c 1s photoionization. However, it turned out that one vibrational progression, i.e., quasi-symmetric stretching mode v_1', was enough to fit the spectrum of Fig. 1.

The N_t 1s photoelectron spectrum of N_2O, in the form of $I(0°) + 2 \times I(90°)$, measured at a photon energy

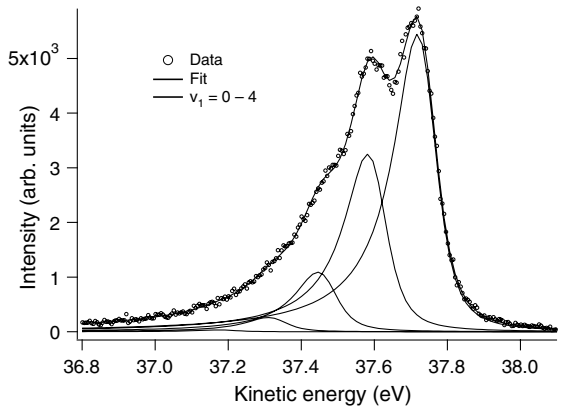

Fig. 1. N_c 1s photoelectron spectrum, $I(0°) + 2 \times I(90°)$, of dinitrogen oxide taken at $h\nu = 450$ eV. Circles – experiment, thick line – modeled spectrum, thin lines – individual peaks.

$h\nu = 450$ eV, is shown in Fig. 2, together with a least-squares curve fitting decompositions into vibrational progressions. Here, two vibrational progressions, both quasi-symmetric and quasi-antisymmetric modes, v_1' and v_3', were needed to obtain a reasonable curve fit. We assumed that the two modes are uncoupled so that

$$E(v_1', v_3') = E(v_1') + E(v_3') - E(0,0). \quad (1)$$

This difference of the vibrational spectra between N_c 1s and N_t 1s ionizations is related to their characteristic geometry relaxation as discussed later. The spectra in Figs. 1 and 2 were fitted simultaneously, using the PCI-distorted line profiles convoluted with the Gaussian profile. The positions of the first peaks ($v_1' = v_3' = 0$) in Figs. 1 and 2, three vibrational frequencies, ω_{e1} for N_c 1s $1s^{-1}$ and ω_{e1} and ω_{e3} for N_t $1s^{-1}$, and the intensities of the individual vibrational components, as well as Lorentzian and Gaussian widths common for all the components, were treated as fitting parameters. The Gaussian width, which represents a convolution of the monochromator bandwidth, electron analyzer bandwidth and Doppler broadening, is ~45 meV, whereas the Lorentzian width Γ is 118 ± 2 meV. The extracted vibrational frequencies are summarized Table 1.

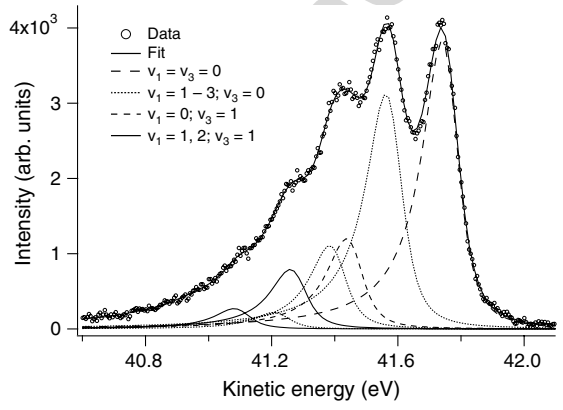

Fig. 2. N_t 1s photoelectron spectrum, $I(0°) + 2 \times I(90°)$, of dinitrogen oxide taken at $h\nu = 450$ eV. Circles – experiment, thick line – modeled spectrum, thin solid, dotted and dashed lines – individual peaks.

Table 1
Vibrational constants, intensity ratios $R(v_1', 0, v_3') \equiv I(v_1', 0, v_3')/I(0, 0, 0)$ and differences of the equilibrium bond lengths between the neutral and ionic species, ΔR_{NN} and ΔR_{NO}, for the N_c and N_t 1s ionized states of N_2O

	Exp. (450 eV)	ECA CCSD(T)		ECA CCSD	Opt.	
N_c $1s^{-1}$						
Γ (meV)	118(2)	–		–	–	
ω_{e1} (meV)	136(2)	125		114	125	
ω_{e3} (meV)	–	225		249	225	
$R(1,0,0)$	0.60(1)	0.467	(0.472)	0.367	0.592	(0.597)
$R(2,0,0)$	0.20(6)	0.110	(0.111)	0.043	0.179	(0.182)
$R(0,0,1)$	–	0.002	(0.004)	0.059	0.007	(0.009)
$R(1,0,1)$	–	0.000	(0.002)	0.003	0.003	(0.005)
ΔR_{NN} (Å)	–	+0.010		−0.007	+0.0125(3)	
ΔR_{NO} (Å)	–	+0.043		+0.045	+0.0485(6)	
N_t $1s^{-1}$						
Γ (meV)	118(2)	–		–	–	
ω_{e1} (meV)	178(1)	175		186	175	
ω_{e3} (meV)	303(2)	295		304	295	
$R(1,0,0)$	0.82(1)	0.840	(0.819)	1.052	0.840	(0.817)
$R(2,0,0)$	0.29(2)	0.301	(0.287)	0.497	0.300	(0.286)
$R(3,0,0)$	0.05(2)	0.061	(0.057)	0.141	0.060	(0.057)
$R(0,0,1)$	0.31(2)	0.276	(0.289)	0.365	0.301	(0.314)
$R(1,0,1)$	0.21(2)	0.192	(0.194)	0.331	0.207	(0.208)
$R(2,0,1)$	0.07(2)	0.055	(0.054)	0.133	0.059	(0.058)
ΔR_{NN} (Å)	–	−0.008		−0.007	−0.0068(9)	
ΔR_{NO} (Å)	–	−0.065		−0.071	−0.0661(9)	

Theoretical calculations using ECA CCSD(T)and ECA CCSD vibrational potentials are compared with the present experimental values. The results for the optimized geometries (Opt.) are also given. For the theoretical $R(v_1', 0, v_3')$ results, both the ratios of Franck–Condon factors and the corresponding intensity ratios from the photoionization calculations are given, with the intensity ratio in the parentheses. See the text for details.

The intensity ratios of the vibrational components can be correlated to the ratios of the Franck–Condon factors only if the excitation energy is sufficiently high, i.e., in the sudden limit. As seen in a separate paper [31], the photon energy 450 eV employed here is not high enough to be completely free from the shape resonance effects. Thus we have computed the ratios obtained from a full photoionization scattering calculation as outlined above using the CCSD(T) potential for the ion states. Both the ratio of Franck–Condon factors and the photoionization ratios are given in Table 1. We can see that for the large branching ratios, the non-Franck–Condon corrections provided by the photoionization calculations amount to a few percent. For the ratios with smaller magnitudes, the corrections are larger on a relative scale, although they are still small on an absolute scale.

The calculated potential energy surface of the N_c 1s ionized state, NOO^+ in ECA, is metastable and dissociative as $NOO^+ \rightarrow NO^+ + O$. The calculated activation barrier for dissociation is only ~0.80 eV considering the zero point energy correction of 0.155 eV, in which bending modes are also included. In Table 1, we presented the vibrational states up to ~0.35 eV relative to the (000) state. The vibrational spectrum by CCSD(T) reasonably agrees with the experimental spectrum. The vibrational excitations are dominantly due to v_1' mode. The vibrational excitations have been underestimated; the calculated vibrational intensity ratios were 0.472 and 0.111 for (100) and (200), respectively, in comparison with the respective experimental values of 0.59 and 0.20. This suggests the underestimate of the geometry change as we discuss later.

For the N_t 1s ionized state, the theoretical spectrum by CCSD(T) satisfactorily agrees with the experimental spectrum. The vibrational frequencies are calculated to be 175 and 295 meV for v_1' and v_3', respectively, in comparison with the experimental values of 178 and 298 meV. The calculated intensity ratios are 0.819, 0.287, 0.289 and 0.194 for (100), (200), (001) and (101), respectively. These values are in reasonable agreement with the experimental ratios of 0.81, 0.27, 0.33 and 0.21, respectively.

5. Discussion

5.1. Ab initio equilibrium geometries

The geometry change in the core-excited state is of particular interest as outlined in the introduction. The geometry change is sensitive to the level of the theoretical calculations. According to the CCSD(T) calculation of the 2D potential energy surfaces, the equilibrium structures of the ground state and core-ionized states are linear. The optimized bond lengths of the ground state are $R_{NN} = 1.133$ and $R_{NO} = 1.190$ Å, which well agree with the experimental values of $R_{NN} = 1.127$ and $R_{NO} = 1.185$ Å [32]. The CCSD(T) calculations indicate that both NN and NO bonds are elongated relative to the ground state, $\Delta R_{NN} = +0.010$ and $\Delta R_{NO} = +0.043$ Å, in the N_c 1s ionized state, as listed in Table 1. For the N_t 1s ionized state, on the other hand, the CCSD(T) calculations predict both NN and NO bonds shrinks, $\Delta R_{NN} = -0.008$, $\Delta R_{NO} = -0.065$ Å, as listed in Table 1: the change in R_{NO} is much larger than that in R_{NN}.

For comparison, we have carried out the calculations using the CCSD method. The basis set employed is the same as that for CCSD(T), i.e. [4s3p2d1f] [29]. The results are given also in Table 1. As for the ground state geometry (not given in Table 1), the CCSD method gives a very reasonable result. In the N_c 1s ionized state, the CCSD within the ECA predicts that NN bond length is shortened, $\Delta R_{NN} = -0.007$, instead elongated, $\Delta R_{NN} = +0.010$, as predicted by CCSD(T). As a consequence, the results for the intensity ratios of the vibrational components are significantly worse than those predicted by CCSD(T). For the N_t 1s ionized state, the CCSD calculations predict a geometry change similar to CCSD(T), though the CCSD frequencies are slightly worse than those predicted by CCSD(T). The CCSD results for the vibrational intensity ratios are significantly worse than in the CCSD(T) approximation. We have also examined the basis-set dependence. It turned out that CCSD/cc-pVQZ gives results that are very similar to the CCSD/cc-pVTZ results. These findings illustrate that inclusion of perturbative triple excitations, CCSD(T), is essential for obtaining reasonable agreement with the experimental results.

As pointed out in the introduction, the use of ECA might cause a significant error in certain cases. We thus discuss the restriction stemming from the ECA in the present case. The N_t 1s ionized state is approximated by the symmetric ONO^+ in ECA. As a result, the calculated bond lengths R_{NN} and R_{NO} are identical in ECA. In order to evaluate the accuracy of this restriction, we have carried out direct calculation of the core–hole state, without using ECA, by the SAC-CI method [33,34]. The basis set employed was cc-pCVDZ [4s3p1d] [35]: the use of a larger basis set was difficult given available computational resources. The calculations were executed with the GAUSSIAN 03 suite of programs [30] with some modifications for calculating the core-ionized states in the SAC-CI program, namely, the reference SDT-CI for core–hole states was enabled. The resulting geometry changes are $\Delta R_{NN} = -0.001$ and $\Delta R_{NO} = -0.062$ Å, or R_{NN} is slightly longer (0.004 Å) than R_{NO}. This direct SAC-CI calculation of the core–hole state, without ECA, suggests that the ECA is approximately valid at least within this accuracy. The vibrational frequencies and vibrational intensity ratios obtained from the SAC-CI 2D potential surfaces (not shown here) are, however, worse than those by CCSD(T) with ECA, indicating that the present SAC-CI calculation with [4s3p1d] is less precise than ECA-CCSD(T) with the larger basis set [4s3p2d1f]. This implies that the SAC-CI results at the present level still suffer from the severe orbital relaxation effect, as discussed in our recent work on C 1s and O 1s ionizations of CO_2 [16]. The CCSD(T) with ECA, on the other hand, is free from orbital relaxation effect as a natural consequence of the ECA.

5.2. Obtaining empirical equilibrium geometries

Using the fact that the vibrational intensity ratios are very sensitive to the change of the equilibrium geometries, we have empirically obtained the equilibrium bond lengths of core ionized states, using the theoretical ECA CCSD(T) 2D potential energy surfaces and vibrational wave functions and regarding the equilibrium bond lengths as fitting parameters.

For the N_c 1s state we have only used the experimental branching ratio $R(1,0,0)$ to obtain the equilibrium structure of the ion. Using only one piece of experimental data implies that we can have only one empirical parameter. The optimization was done in this case using the normal modes

of the initial state. We fixed the change in the v_3' quasi-antisymmetric mode from the ground to the ion state to be that obtained by the CCSD(T) calculations and only treated the change in the v_1' quasi-symmetric modes as an empirical parameter. The change of the bond lengths found with this empirical optimization, given in Table 1, are $\Delta R_{NN} = +0.0125(3)$ and $\Delta R_{NO} = +0.0485(6)$ Å. The estimated uncertainties in these quantities are obtained using the estimated experimental uncertainty in the $R(1,0,0)$ branching ratio of 0.01. It is worth noting that the change of R_{NO} is much larger than that of R_{NN}. We also note that this shift in geometry is close to that found in the CCSD(T) calculation: the optimized values for ΔR_{NN} and ΔR_{NO} were slightly larger by 0.002 Å and 0.005 Å, respectively, than the CCSD(T) results. This small change, however, causes a fairly significant change in the $R(1,0,0)$ intensity ratio from 0.472 in the CCSD(T) case to 0.597 in the optimized potential.

For the N_t 1s state, the corresponding optimized potential was obtained fitting the experimental values of $R(1,0,0)$ and $R(0,0,1)$ while adjusting both of the equilibrium bond lengths R_{NN} and R_{NO}. The optimized geometry had $\Delta R_{NN} = -0.0068(9)$ Å and $\Delta R_{NO} = -0.0661(9)$ Å with a symmetric geometry to within the experimental uncertainty with $R_{NN} - R_{NO} = 0.0015(18)$ Å. The value of $R_{NN} - R_{NO}$ in the optimized potential is predominantly controlled by the value of $R(0,0,1)$, so that the fairly large uncertainty in $R_{NN} - R_{NO}$ is determined by the experimental uncertainty of 0.02 in $R(0,0,1)$. The value of $R_{NN} + R_{NO}$ in the N_t 1s state is controlled by the value of $R(1,0,0)$ and has the value $R_{NN} + R_{NO} = 2.2395(6)$ Å. It is interesting to note that the terminal N 1s ionization has a larger effect on R_{NO} than on R_{NN}.

6. Conclusion

From the N_c and N_t 1s photoelectron spectra of N_2O measured at high resolution we have extracted vibrational frequencies and intensity ratios for the N_c and N_t 1s ionized states. Vibrational frequencies obtained from the 2D potential surfaces calculated by the CCSD(T) method within the equivalent core approximation agree well with the experimental values. The vibrational intensity ratios computed by the MCSCI method employing the ab initio 2D potential energy surfaces also agree well with the experimental values. The CCSD gives poorer results, indicating the importance of the inclusion of the perturbative triple, CCSD(T). The validity of the ECA was evaluated with the help of SAC-CI calculation of the core–hole state. The equilibrium geometries of the core–hole states were also determined from the experimental vibrational intensity ratios, using the MCSCI calculations and treating the equilibrium bond lengths as fitting parameters. Knowing these geometries is essential in the ab initio calculations for the photoionization cross sections as will be discussed in detail in a separate letter [31].

Acknowledgements

The experiment was carried out with the approval of the SPring-8 program review committee. This study was supported by a Grant for Creative Scientific Research from the Ministry of Education, Science, Culture and Sports of Japan and by Grants-in-Aid for Scientific Research from the Japanese Society for the Promotion of Science (JSPS). The authors are grateful to T.D. Thomas for helpful comments and the staff of the SPring-8 for assistance during the experiment. J.S. acknowledges Tohoku University for hospitality and financial support during his stay. R.R.L. gratefully acknowledge the support of the JSPS through a Fellowship for Research and the hospitality of the Tohoku University. R.R.L. also acknowledges the support of the Robert A. Welch Foundation (Houston, TX) under grant A-1020.

References

[1] L.S. Cederbaum, W. Domcke, Adv. Chem. Phys. 36 (1977) 205.
[2] J. Müller, H. Ågren, in: J. Berkovitz, K.-O. Groeneveld (Eds.), Proceedings of the NATO Advanced Study Institute on Molecular Ions (Kos, Greece), vol. B 90, Plenum, New York, 1980, p. 221.
[3] L. Asplund, U. Gelius, S. Hedman, K. Helenelund, K. Siegbahn, P.-E.-M. Siegbahn, J. Phys. B: At. Mol. Opt. 18 (1985) 1569.
[4] J.D. Bozek, G.M. Bancroft, J.N. Cutler, K.H. Tan, Phys. Rev. Lett. 64 (1990) 2757.
[5] U. Hergenhahn, J. Phys. B: At. Mol. Opt. Phys. 37 (2004) R89, and references therein.
[6] N.V. Dobrodey, H. Köppel, L.S. Cederbaum, Phys. Rev. A 60 (1999) 1988.
[7] T. Karlsen, K.-J. Borve, J. Chem. Phys. 112 (2000) 7986.
[8] T.-X. Carroll, N. Berrah, J. Bozek, J. Hahne, E. Kukk, L.-J. Saethre, T.-D. Thomas, Phys. Rev. A 59 (1999) 3386.
[9] K. Ueda, J. Phys. B: At. Mol. Opt. Phys. 36 (2003) R1, and references therein.
[10] K.J. Borve, L.J. Sæthre, T.D. Thomas, T.X. Carroll, N. Berrah, J.D. Bozek, E. Kukk, Phys. Rev. A 63 (2001) 012506.
[11] T. Karlsen, L.J. Sæthre, K.J. Borve, N. Berrah, J.D. Bozek, T.X. Carroll, T.D. Thomas, J. Phys. Chem. A 105 (2001) 7700.
[12] R. Sankari et al., Chem. Phys. Lett. 380 (2003) 647.
[13] K. Ueda et al., Phys. Rev. Lett. 243004 (2005) 94.
[14] M. Matsumoto et al., Chem. Phys. Lett. 417 (2006) 89.
[15] M. Ehara et al., J. Chem. Phys. 124 (2006) 124311.
[16] T. Hatamoto et al., J. Electr. Spectrosc. Relat. Pheonom, in press.
[17] M. Alagia et al., Phys. Rev. A 71 (2005) 012506.
[18] T.D. Thomas, L.J. Sæthre, S.L. Sorensen, S. Svensson, J. Chem. Phys. 109 (1998) 1041.
[19] M.N.R. Wohlfarth, L.S. Cederbaum, J. Chem. Phys. 116 (2002) 8723.
[20] N.V. Kryzhevoi, N.V. Dobrodey, L.S. Cederbaum, J. Chem. Phys. 118 (2003) 2081.
[21] R.R. Lucchese, K. Takatsuka, V. McKoy, Phys. Rep. 131 (1986) 147.
[22] R.E. Stratmann, R.R. Lucchese, J. Chem. Phys. 102 (1995) 8493.
[23] R.E. Stratmann, R.W. Zurales, R.R. Lucchese, J. Chem. Phys. 104 (1996) 8989.
[24] T. Tanaka, H. Kitamura, J. Synchrotr. Radiat. 3 (1996) 47.
[25] H. Ohashi et al., Nucl. Instrum. Meth. A 467 (2001) 529.
[26] H. Ohashi et al., Nucl. Instrum. Meth. A 467 (2001) 533.
[27] Y. Shimizu et al., J. Electron Spectrosc. Relat. Phenom. 114–116 (2001) 63.
[28] H. Yoshida et al., AIP Conf. Proc. 705 (2004) 267.
[29] T.H. Dunning Jr., J. Chem. Phys. 90 (1989) 1007.

[30] M.J. Frisch et al., GAUSSIAN 03, Rev. C.02, Gaussian Inc., Wallingford, CT, 2004.
[31] J. Söderström et al., in preparation.
[32] J.L. Teffo, A. Chedin, J. Mol. Spectrosc. 135 (1989) 389.
[33] H. Nakatsuji, Computational Chemistry – Review of Current Trends, vol. 2, World Scientific, 1997, p. 62.
[34] M. Ehara, J. Hasegawa, H. Nakatsuji, SAC-CI Method Applied to Molecular Spectroscopy, in: C.E. Dykstra, G. Frenking, K.S. Kim, G.E. Scuseria (Eds.), Theory and Applications of Computational Chemistry: The First 40 Years, Elsevier, Oxford, 2005, p. 1099.
[35] D.E. Woon, T.H. Dunning Jr., J. Chem. Phys. 103 (1995) 4572.